Can aliphatic anchoring groups be utilised with dyes for p-type dye sensitized solar cells?

Yan Hao,[a†] Christopher J. Wood,[†b,c] Charlotte A. Clark,[b] James A. Calladine,[b] Raphael Horvath,[b] Magnus W. D. Hanson-Heine,[b] Xue-Zhong Sun,[b] Ian P. Clark,[e] Michael Towrie,[e] Michael W. George*,[b,d] Xichuan Yang,[a*] Licheng Sun,[a.f] Elizabeth A. Gibson*[b,c]

[a] *DUT-KTH Joint Research Centre on Molecular Devices, State Key Laboratory of Fine Chemicals, Dalian University of Technology (DUT), Dalian, China.*

[b] *School of Chemistry, The University of Nottingham, University Park, Nottingham, NG7 2RD, UK.*

[c] *Now at School of Chemistry, Newcastle University, Newcastle upon Tyne, NE1 7RU, United Kingdom.*

[d] *Department of Chemical and Environmental Engineering, University of Nottingham Ningbo China, 199 Talking East Road, Ningbo 315100, China.*

[e] *Central Laser Facility, Research Complex at Harwell, Science and Technology Facilities Council, Rutherford Appleton Laboratory, Harwell Oxford, Didcot, Oxfordshire, OX11 0QX, United Kingdom*

[f] *KTH Royal Institute of Technology, Department of Chemistry, 10044 Stockholm, SE 10044, Sweden.*

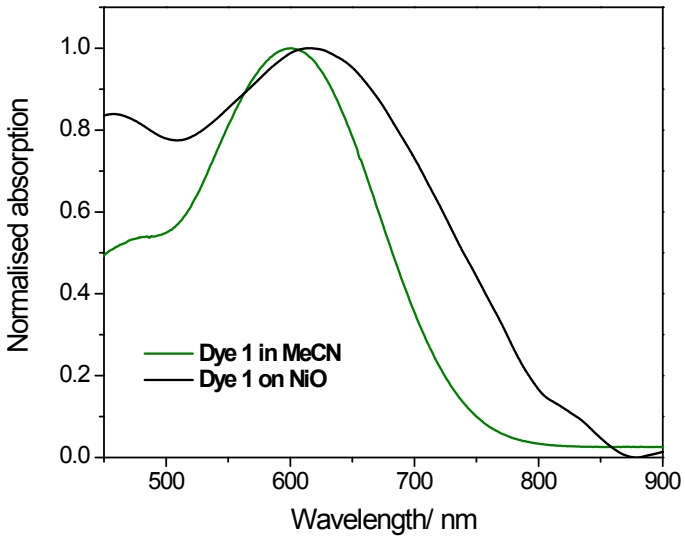

Figure S1. Normalised absorption spectra of **Dye 1** in CH_2Cl_2 solution and adsorbed onto NiO.

Table S1. Comparison of key ground state IR frequencies for **Dye 1** in a KBr pressed disc and adsorbed on mesoporous NiO**.**

Wavenumber (cm^{-1})		
KBr	**NiO**	**Shift**
1072	1079	7
1110	1114	4
1186	1189	3
1205	1207	2
1251	1261	10
1269	1282	13
1283	1282	-1
1348	1352	4
1375	1377	2
1392	1390	-2
1444	1447	3
1474	1478	4
1525	1535	10
1536	1547	11
1751	-	Absent
2209	-	Absent
2227	2227	

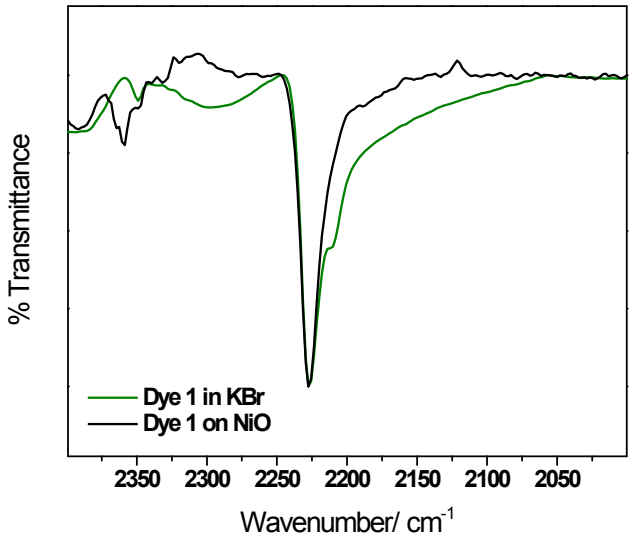

Figure S2. FTIR spectra of **Dye 1** in a KBr disk (green) and **Dye 1**|NiO (black), zoomed in at 2000-2400 cm^{-1} .

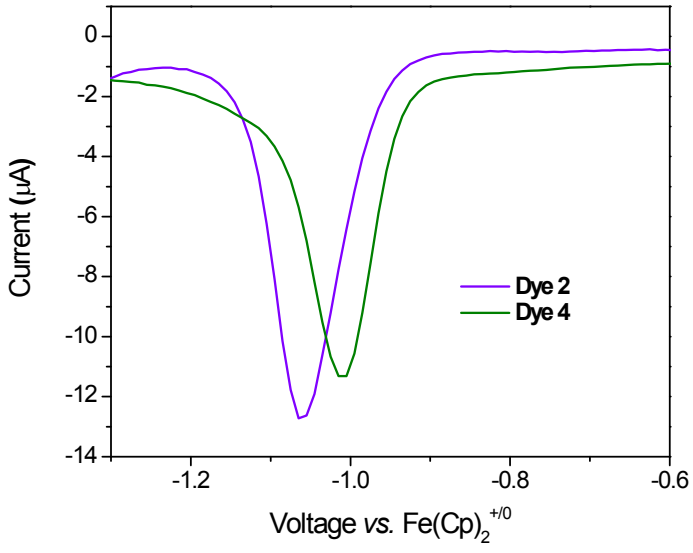

Figure S3. Differential pulse voltammograms for the reduction of **Dyes 2 & 4** measured in CH_3CN with 100 mM $^tBu_4NPF_6$ as the supporting electrolyte (working electrode: glassy carbon; reference electrode: Ag/Ag^+ ; calibrated with $Fe(Cp)_2^{+/0}$ as an external reference, counter electrode: platinum mesh).

Table S2. Approximate driving forces for injection and regeneration for **Dyes 1-4** adsorbed on mesoporous NiO**.** ΔG_{inj} and ΔG_{reg} are estimated from Equation S1 and Equation S3 respectively.

Dye	ΔG /eV (MeCN)	
	Inj(NiO)	**Reg(NiO)**
Dye 1	0.775	0.245
Dye 2	0.795	0.245
Dye 3	0.79	0.19
Dye 4	0.78	0.19

Equation S1. $$\Delta G_{inj} = e[E_{VB}(NiO) - E_{(D^*/D^-)}]$$

Equation S2. $$E_{(D^*/D^-)} = E_{(D/D^-)} + E_{0-0}$$

Equation S3. $$\Delta G_{reg} = e[E_{(D/D^-)} - E(I_3^-/I\cdot_2^-)]$$

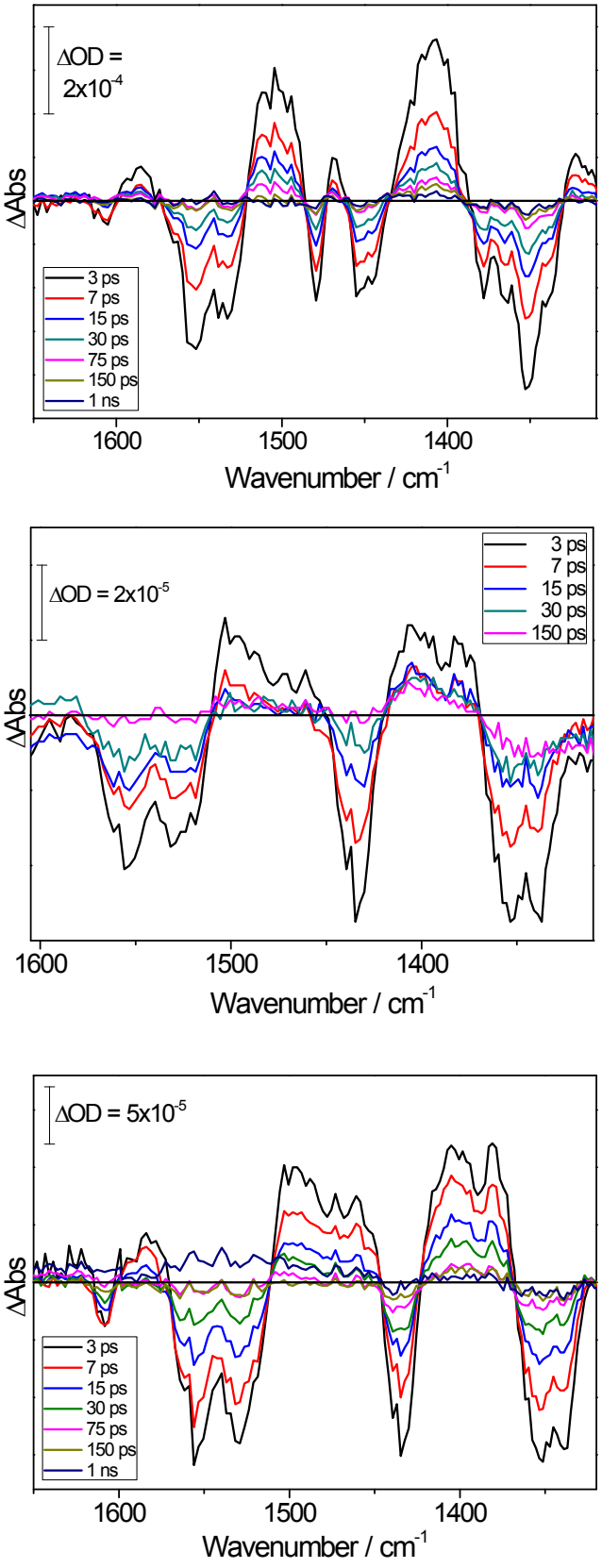

Figure S4. ps-TRIR spectra at selected delays of **Dye 2** (top), **Dye 3** (middle) and **Dye 4** (bottom).

Table S3. Band positions observed from TRIR measurements for ground state and reduced state for each of the dyes adsorbed on NiO.

Dye	**Wavenumber / cm^{-1}**	
	Ground State	Anion
Dye 1	1605	1585
	1544	1508
	1477	1475
	1447	1414
	1353	1320
Dye 2	1610	1588
	1546	1509
	1489	1476
	1455	1415
	1362	1321
Dye 3	1540	1591
	1434	1480
	1346	1400
		1377
Dye 4	1607	1587
	1541	1478
	1435	1404
	1348	1381

Table S4. Scaled harmonic vibrational frequencies (in cm^{-1}) and infrared intensities (km/mol) in the spectral region between 1200 and 3000 cm^{-1} for **Dye 1** in its neutral and anionic forms. Calculated *in vacuo* at the B3LYP/6-311G(d,p) level of theory. Frequencies have been scaled by 0.9682.

Neutral Form		**Anionic Form**	
Frequencies	**Intensities**	**Frequencies**	**Intensities**
1206	54.59	1208	123.00
1208	7.96	1214	2.76
1214	182.74	1224	25.87
1229	13.71	1230	6.84
1240	28.89	1232	27.54
1245	14.03	1243	27.98
1249	9.73	1246	0.52
1254	40.97	1255	24.95
1259	95.81	1257	25.52
1275	648.96	1266	183.58
1276	351.23	1270	168.23
1285	20.91	1282	31.18
1296	65.60	1292	9.38
1301	296.26	1311	145.07
1316	111.43	1314	10.76
1317	44.78	1321	40.25
1324	8.12	1325	100.88
1334	112.07	1335	81.64
1340	56.35	1340	36.55
1345	327.73	1350	245.19
1348	186.11	1350	6.26
1355	62.24	1354	12.97
1357	720.08	1355	19.07
1362	11.75	1364	34.96
1368	365.53	1369	47.58
1371	16.69	1372	5.57
1375	2.32	1378	25.64
1383	282.91	1388	348.49
1391	59.60	1399	95.33
1427	21.09	1421	104.90
1429	740.95	1425	18.04
1432	1.62	1426	375.18
1434	72.70	1432	1.97
1435	13.21	1434	168.63
1436	2.14	1435	0.02
1439	33.23	1436	4.09
1440	403.23	1441	0.62
1446	314.57	1445	7.46
1447	13.67	1447	5.00

1451	3.37	1447	4.45
1451	18.81	1449	14.05
1455	1.67	1453	16.81
1459	11.57	1455	44.72
1460	12.44	1459	12.88
1460	18.04	1459	10.10
1463	19.14	1461	7.86
1464	33.82	1462	66.16
1467	667.47	1466	28.93
1481	50.22	1479	380.64
1494	59.49	1487	250.12
1508	24.05	1501	2224.08
1522	65.44	1525	129.40
1541	1466.46	1527	129.15
1548	115.04	1539	80.88
1580	239.63	1593	44.10
1592	192.82	1752	274.93
1749	274.57	2211	141.74
2247	34.35	2219	157.60
2257	11.99	2236	630.48
2263	196.95	2858	123.14
2885	97.14	2886	23.88
2895	14.87	2915	42.82
2928	6.52	2926	6.31
2932	28.55	2928	61.00
2936	26.27	2930	34.78
2939	34.80	2932	29.11
2943	38.81	2939	58.91
2952	7.56	2941	14.70
2956	7.46	2945	30.95
2956	17.50	2947	22.30
2960	28.38	2951	28.75
2968	11.62	2963	32.05
2972	27.82	2965	54.60
2973	36.95	2987	61.33
2993	48.57	2991	5.79
2997	24.04	2997	68.47
2999	4.84	2999	32.91

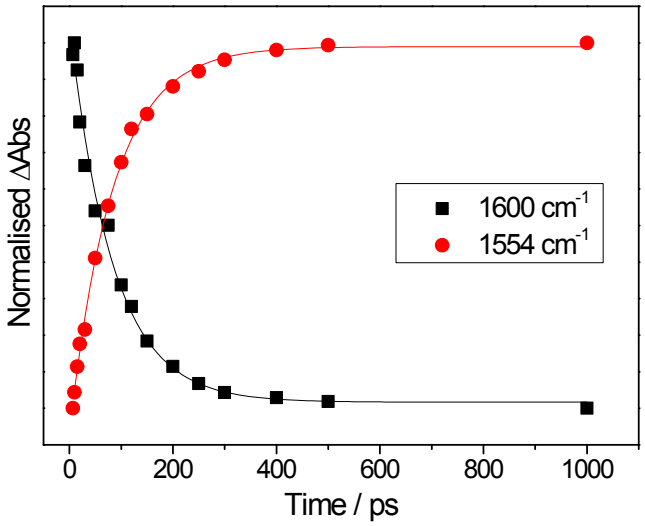

Figure S5. – Kinetic trace recorded from TRIR showing decay of excited state band at 1600 cm^{-1} and recovery of parent band at 1554 cm^{-1}.

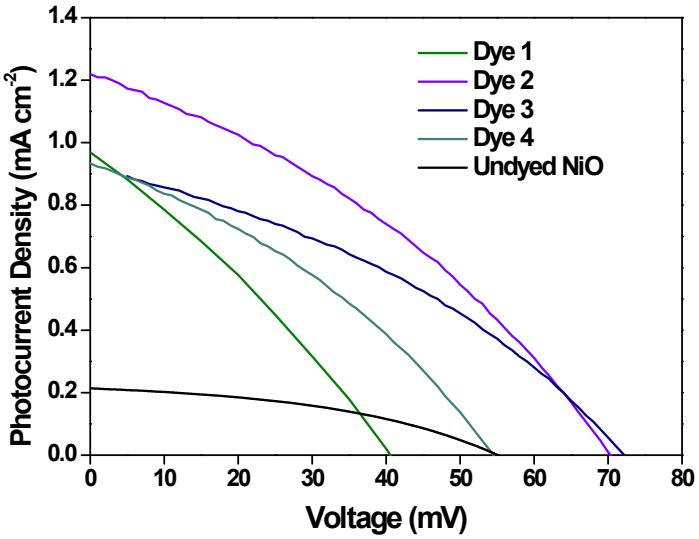

Figure S6. Photocurrent density-voltage curves for NiO p-DSCs sensitized by **Dyes 1-4** with blank NiO included for comparison.

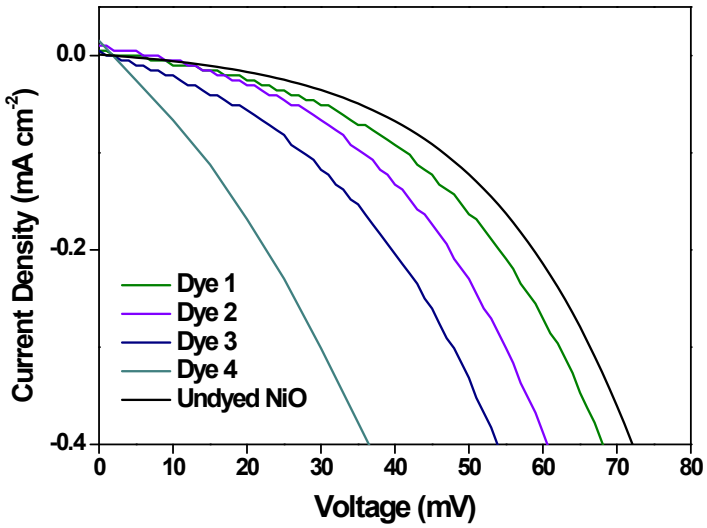

Figure S7. Dark current curves for NiO p-DSCs sensitized by **Dyes 1-4** with blank NiO included**.**

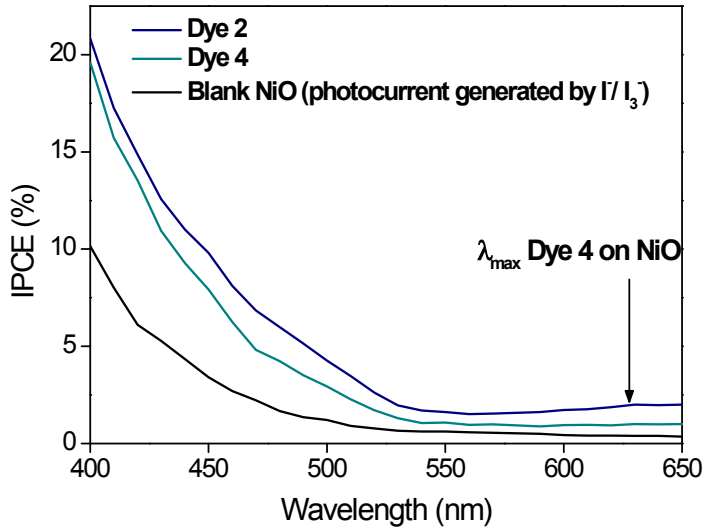

Figure S8. IPCE spectra for NiO p-DSCs sensitized by the **Dyes 2 & 4** and without dye.

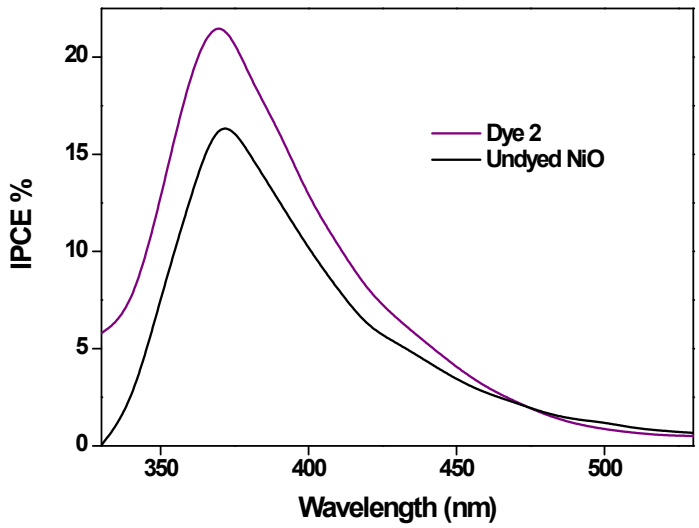

Figure S9. IPCE spectra for NiO p-DSCs sensitized by the **Dye 2** and without dye measured to 330 nm.

References

1 Y. Shao, L. F. Molnar, Y. Jung, J. Kussmann, C. Ochsenfeld, S. T. Brown, A. T. B. Gilbert, L. V. Slipchenko, S. V. Levchenko, D. P. O'Neill, R. a DiStasio, R. C. Lochan, T. Wang, G. J. O. Beran, N. A. Besley, J. M. Herbert, C. Y. Lin, T. Van Voorhis, S. H. Chien, A. Sodt, R. P. Steele, V. A. Rassolov, P. E. Maslen, P. P. Korambath, R. D. Adamson, B. Austin, J. Baker, E. F. C. Byrd, H. Dachsel, R. J. Doerksen, A. Dreuw, B. D. Dunietz, A. D. Dutoi, T. R. Furlani, S. R. Gwaltney, A. Heyden, S. Hirata, C.-P. Hsu, G. Kedziora, R. Z. Khalliulin, P. Klunzinger, A. M. Lee, M. S. Lee, W. Liang, I. Lotan, N. Nair, B. Peters, E. I. Proynov, P. A. Pieniazek, Y. M. Rhee, J. Ritchie, E. Rosta, C. D. Sherrill, A. C. Simmonett, J. E. Subotnik, H. L. Woodcock, W. Zhang, A. T. Bell, A. K. Chakraborty, D. M. Chipman, F. J. Keil, A. Warshel, W. J. Hehre, H. F. Schaefer, J. Kong, A. I. Krylov, P. M. W. Gill and M. Head-Gordon, *Phys. Chem. Chem. Phys.*, 2006, **8**, 3172–3191.

2 A. D. Becke, *J. Chem. Phys*, 1993, **98**, 5648–5652.

3 F. J. Devlin, J. W. Finley, P. J. Stephens and M. J. Frisch, *J. Phys. Chem*, 1995, **99**, 16883–16902.

4 J. P. Merrick, D. Moran and L. Radom, *J. Phys. Chem. A*, 2007, **111**, 11683–11700.

5 I. P. Clark, M. W. George, G. M. Greetham, E. C. Harvey, C. Long, J. C. Manton and M. T. Pryce, *J. Phys. Chem. A*, 2011, **115**, 2985–2993.

6 G. M. Greetham, P. Burgos, Q. Cao, I. P. Clark, P. S. Codd, R. C. Farrow, M. W. George, M. Kogimtzis, P. Matousek, A. W. Parker, M. R. Pollard, D. A. Robinson, Z.-J. Xin and M. Towrie, *Appl. Spec.*, 2010, **64**, 1311–1319.